Distribution of resonances in the quantum open baker map

Juan M. Pedrosa,[1] Gabriel G. Carlo,[1] Diego A. Wisniacki,[2] and Leonardo Ermann[1,2]
[1]*Departamento de Física, CNEA, Av. Libertador 8250, C1429BNP Buenos Aires, Argentina*
[2]*Departamento de Física, FCEyN, UBA, Pabellón 1 Ciudad Universitaria, C1428EGA Buenos Aires, Argentina*
(Received 5 November 2008; published 23 January 2009)

We study relevant features of the spectrum of the quantum open baker map. The opening consists of a cut along the momentum p direction of the 2-torus phase space, modeling an open chaotic cavity. We study briefly the classical forward trapped set and analyze the corresponding quantum nonunitary evolution operator. The distribution of eigenvalues depends strongly on the location of the escape region with respect to the central discontinuity of this map. This introduces new ingredients to the association among the classical escape and quantum decay rates. Finally, we could verify that the validity of the fractal Weyl law holds in all cases.

DOI: 10.1103/PhysRevE.79.016215 PACS number(s): 05.45.Mt, 03.65.Sq

I. INTRODUCTION

Recently, there has been an upsurge of the interest in open quantum systems, whose properties are still less known compared to those of the closed ones. Besides their general fundamental importance, they are also of the utmost relevance in very active fields. We can mention a few of them, such as the study of the quantum to classical correspondence [1], quantum dots [2], microlasers having chaotic resonant cavities [3–5], and chaotic scattering [6,7]. These systems are characterized by a nonunitary quantum evolution. The corresponding operators have a set of right and left decaying nonorthogonal eigenfunctions associated to them. Their complex eigenvalues z_i (also referred to as resonances) fall inside the unit circle when represented in the complex plane, i.e., $\nu_i^2=|z_i|^2=\exp(-\Gamma_i)\leqslant 1$. The exponent $\Gamma_i \geqslant 0$ is the usually called decay rate.

The classical phase space of open chaotic systems is characterized by fractal sets associated with trajectories that remain trapped for infinite times. Those orbits that stay forever in the future define what it is called the forward trapped set, and those that stay forever in the past define the backward one. An initial classical probability uniformly distributed in the phase space decays at an exponential rate. This allows us to define the so-called classical escape rate γ_{cl}. The intersection of both sets, that is, the set of trajectories which do not escape to infinity either in the past or in the future is called the repeller.

Regarding the eigenstates, we can distinguish between short-lived and long-lived ones. The former ($\Gamma_i \gg 1$) are associated with the trajectories that escape from the system before the Ehrenfest time, while the latter [$\Gamma_i = O(1)$] are related to the classical trapped sets, thus carrying the most relevant classical information. One of the most important properties of open quantum systems is the conjectured fractal Weyl law. This law relates the mean density of resonances, $\hbar$ and the structure of the classical phase space. It predicts that the number of long-lived states goes as $N_\gamma \sim \hbar^{-(d-1)}$, where d is a fractal dimension of the classical strange repeller. This law has been checked for a three disk system [8] and some quantum maps [9–14], and it is still being tested. But much less is known about the distribution of the resonances. There are some results obtained for random matrix models [15]. Also, a scaling property has been numerically verified for the open kicked rotator [9]. Essentially, the classical escape rates of this system determine the quantum decay rates associated with the long-lived eigenstates. However, there are no analytical results for the semiclassical limiting distribution. We shed light into this open problem by concentrating on the spectral behavior of the most simple models of open chaotic dynamics, i.e., open piecewise linear maps. Discontinuities are an essential part of these systems, being responsible for their chaoticity. Then it is very interesting to study their influence on the spectral behavior.

In this work we focus on the quantum open baker map, which is a chaotic transformation of the unit square (2-torus) phase space. This is a paradigmatic model in classical and quantum chaos and also in statistical mechanics [6,16]. Its relevance both, in fundamental studies and in applications to a wide range of areas, is difficult to overestimate. As such, a deep knowledge of its spectral features is very important. We have investigated the behavior of the distribution of its eigenvalues as a function of the location of the escape region in phase space. We have found that the central discontinuity of this map plays a crucial role in the behavior of the spectrum. The quantum effects can be related to the classical behavior, which we study very briefly in order to support our explanations. But there are also important features of purely quantum character. In fact, the link between the classical escape and the quantum decay rates is more subtle for openings that overlap with the central discontinuity of our map than for those which do not. The shortest periodic orbits become relevant in the overlapping cases and based on this we provide a conjecture in order to explain our finding.

This paper is structured as follows: In Sec. II we describe the model, giving a short introduction to the classical dynamics and the quantization method used. In Sec. III we first study some aspects of the classical dynamics that help us to understand the spectral behavior. Then we show the results for the distribution of eigenvalues and present a conjecture explaining them. We also verify the validity of the fractal Weyl law for all cases under investigation. Finally, in Sec. IV we draw the conclusions.

II. CLASSICAL AND QUANTUM OPEN BAKER MAP

In this section we introduce the main features of two-dimensional torus open maps and define our system. We use

a very simple method to model dissipation as it occurs in scattering through a cavity, for instance. We assume that all the classical initial conditions that are mapped inside the area of phase space corresponding to the opening leave the system. Thus, the open map is defined on a subset of the 2-torus. If we choose an opening that represents a fraction M/N of the total area in phase space, then the open quantum map corresponds to a nonunitary matrix $B^o=BP$. In this expression, P is a projector onto the complement of the opening, and the operator B corresponds to the closed quantum map, a unitary matrix acting on a Hilbert space of dimension $N=1/2\pi\hbar$.

We study the open baker map with different opening sizes along the p direction. The closed classical transformation is defined in the 2-torus $\mathcal{T}^2=[0,1)\times[0,1)$ by

$$\mathcal{B}(q,p)=\begin{cases}(2q,p/2) & \text{if } 0\leqslant q<1/2,\\ (2q-1,(p+1)/2) & \text{if } 1/2\leqslant q<1.\end{cases} \tag{1}$$

This transformation is an area-preserving, uniformly hyperbolic, piecewise-linear, and invertible map with Lyapunov exponent $\lambda=\ln 2$. Geometrically, the map stretches the unit square by a factor of 2 in the q direction, squeezes it by the same factor in the p direction, and then stacks the right half onto the left one. The opening is performed by eliminating from the evolution those initial conditions falling inside a rectangle of width Δq, centered at q_c and extending along the whole p axis in phase space. The dynamics of the open baker map has been previously studied [17,18]. However, the role played by discontinuities (especially the one along the line $q=1/2$) has not received much attention. Moreover, we do not know of any study regarding its effects on the spectral behavior of the quantum version.

Following the quantization process described in [16,19], in an even N-dimensional Hilbert space, the quantum baker map is defined in terms of the discrete Fourier transform in the position representation as

$$B_N=G_N^{-1}\begin{pmatrix}G_{N/2} & 0\\ 0 & G_{N/2}\end{pmatrix}, \tag{2}$$

with

$$(G_N)_{jk}=\frac{1}{\sqrt{N}}\exp[-2\pi i(j+1/2)(k+1/2)/N].$$

B_N is a unitary matrix and represents the quantum dynamics of the closed baker map. A Δq wide cut is made along the p direction by means of the projector operator P on its complement. Finally, the corresponding quantum dynamics for the open baker map is given by the nonunitary matrix $B_N^o=B_NP$. It is worth mentioning that we have chosen to open the baker map in a different way than in [11,12]. This allows us to vary the location and width of the escape region.

III. EIGENVALUES: THE ROLE OF DISCONTINUITIES

A. Classical repeller

We first study some features of the classical phase space of our system. This is solely intended to understand which

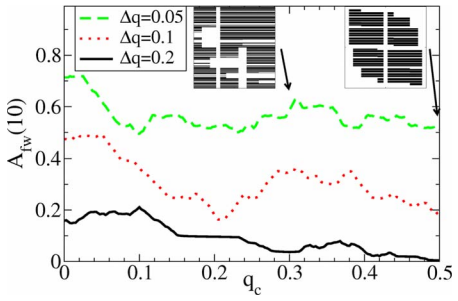

FIG. 1. (Color online) Area of the forward trapped set for the tenth iteration of the open baker map $A_{fw}(10)$ as a function of the center of the opening q_c for different widths, with $\Delta q=0.2$ (black solid line), $\Delta q=0.1$ (red dotted line), and $\Delta q=0.05$ (green dashed line). The insets show the forward trapped sets (in black) for $t=10$ and $\Delta q=0.05$, for $q_c=0.3$ (left-hand side) and $q_c=0.5$ (right-hand side).

are the main classical ingredients that play a significant part quantum mechanically. These ingredients will help in the explanation of the quantum behavior, which is the main interest of this work. For that purpose, we have calculated the escape rate for different locations and sizes of the opening. By means of the area of the forward trapped sets as a function of the number of the iterations of the map $A_{fw}(t)$, the classical escape rate can be easily calculated as $\gamma_{cl}=-\ln A_{fw}(t)/t$. Then, the information dimension d_I of the corresponding repeller can be determined through the known relationship $d_I=2-\gamma_{cl}/\lambda$ [6,20,21].

In Fig. 1 we can see the value of $A_{fw}(10)$, i.e., the area of the tenth iteration of the map as a function of the position of the center of the opening q_c, for three different values of the width, $\Delta q=0.05$, 0.1, and 0.2. Given that this quantity is symmetrical with respect to $q_c=0.5$ (for a given Δq), we only show values in the range $q_c\in[0;0.5]$. In order to calculate these curves we have evolved initial conditions uniformly covering the phase space, eliminating the area corresponding to the opening at each iteration.

It can be clearly noticed that there is a common shape regardless of the size of the escape region. The minimum of A_{fw} is at $q_c=0.5$, while the maximum is generally at $q_c=0$. Also, we can identify a minimum at $q_c\sim0.25$ and a maximum at $q_c\sim0.3$. This can be roughly explained by means of the first iterations of the opening through the map. In fact, the openings located at the central discontinuity typically do not overlap with their first iterations since there are no periodic orbits at $q=0.5$. As a result, initial conditions escape faster. This is not the case when the cut is made at the discontinuity at $q=0$, which includes the shortest periodic orbit ($q=0$, $p=0$). As a consequence, an opening overlapping with this discontinuity behaves much in the same way as one having a generic q_c value. We have found that it is possible to use the shortest periodic orbits to give a good estimate for the main features of these curves (this will be explained elsewhere [22]). In the insets we can see two examples of the shape of the forward trapped sets at $q_c=0.3$ and $q_c=0.5$ for $\Delta q=0.05$. These two positions of the escape region illustrate the two most relevant situations: In the first case the opening is far from the central discontinuity of the map and its first

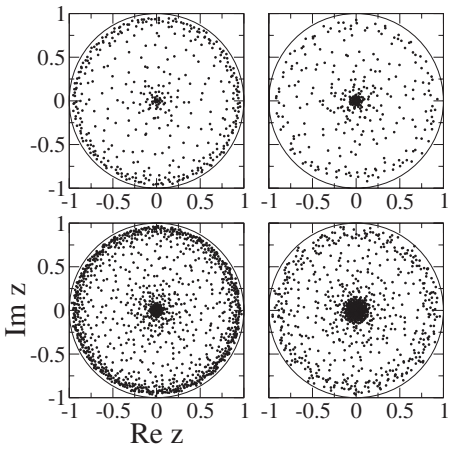

FIG. 2. Eigenvalues of the open baker map in the complex plane. In the upper panels we show the case for $N=602$ and in the lower ones for $N=2048$. In the left-hand panels the opening is centered at $q_c=0.3$ and in the right-hand ones at $q_c=0.5$; $\Delta q=0.1$ in all cases.

iterations, while in the second case it is centered on it. The maximum escape rate is reached for this latter and this can be easily associated with the thinner look of the phase space distribution. We have calculated the escape rates for $\Delta q=0.1$ with $q_c=0.3$ and $q_c=0.5$, resulting in $\gamma_{cl}=0.090\,73$ and $\gamma_{cl}=0.164\,88$, respectively. The corresponding information dimensions are $d_I=1.869\,10$ and $d_I=1.762\,13$. In the following we will see how this behavior translates into the quantum domain.

B. Eigenvalues

We now study the behavior of the distribution of the eigenvalues of the quantum evolution operator. We first show the eigenvalues in the complex plane for $\Delta q=0.1$. As can be seen in Fig. 2, since moduli are less than one ($\nu<1$) all of them fall inside the unit circle. They cluster near the origin and at a ring close to $\nu=1$. In the upper panels $N=602$, while in the lower ones $N=2048$. In both cases we display the results for $q_c=0.3$ on the left-hand side and $q_c=0.5$ on the right-hand side. In these last situations there is a much less dense distribution of eigenvalues at the outer ring, and an increase of density near the origin. This is consistent with the predictions of the fractal Weyl law, given that the information dimension of the classical repeller is smaller for $q_c=0.5$. It is interesting to mention that for an opening at $q_c=0$ the behavior is rather similar to what happens for one at a q_c far from discontinuities.

To gain further insight about the behavior of this distribution, we have calculated the normalized cumulative number of resonances $n=i/N$ as a function of ν. In Fig. 3 results for the same values of Δq, N, and q_c as in Fig. 2 can be seen (see caption for details). From this figure it is clear that there is a higher density of eigenvalues near $\nu=0$ for $q_c=0.5$, and a lower density near $\nu=1$ for $q_c=0.3$. Also, the shape of the tails ($\nu\gtrsim 0.7$) of both distributions seems to be different, showing a more linear behavior in the former rather than in the latter case.

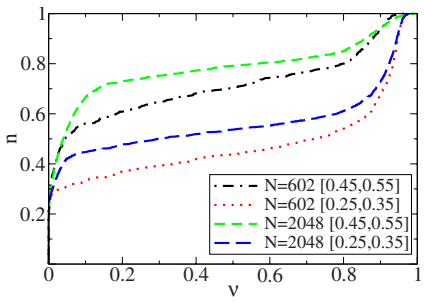

FIG. 3. (Color online) Cumulative number of resonances n as a function of ν. The green short dashed line corresponds to $N=2048$ and the black dotted-dashed line corresponds to $N=602$, both for $q_c=0.5$; the blue long dashed line corresponds to $N=2048$ and the red dotted line corresponds to $N=602$, both for $q_c=0.3$.

In order to better evaluate the eigenvalue distribution we have constructed the histograms for $W=dn/d\nu$ where the bin size has been taken as $\Delta\nu=0.01$. We show values for $\nu>0.7$, corresponding to the tails of Fig. 3. To compare the distributions W at different relevant cases, we have constructed Fig. 4. In these plots we have superimposed the cases for $q_c=0.3$ and $q_c=0.5$. In the upper panel the $N=2048$ case can be seen. This is an example of the special situation for the baker map when the dimension is of the form $N=2^l$, where l is an integer number. In the middle panel we can see an example for $N=602$ (in this case $N\neq 2^l$) where the width for $q_c=0.5$ is much greater than that for $q_c=0.3$. In the lower panel there is an example for $N=1782$ that shows a smaller width, now for the $q_c=0.5$ case.

It is clear from Fig. 4 that the width of W can vary significantly with N. To have a complete picture of this behavior we have also computed the width σ of the eigenvalue distributions as a function of the dimension of the Hilbert space in the interval $N\in[500;2000]$, for $\Delta q=0.1$. We have numerically measured the width of each histogram at one-half height for $\nu>0.7$. Results are shown in Fig. 5, where we have taken $q_c=0.3$ and 0.5. We can see that the widths of the distributions are similar for a wide range of Hilbert space dimensions. They are generally greater for $q_c=0.5$ than for $q_c=0.3$ by approximately a factor of 1.5. However, there are

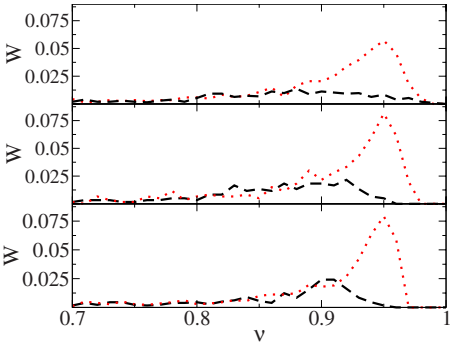

FIG. 4. (Color online) Histograms corresponding to the eigenvalue distribution W as a function of ν for $q_c=0.3$ (red dotted lines) and $q_c=0.5$ (black dashed lines). In the upper panel $N=2048$, in the middle panel $N=602$, and in the lower panel $N=1782$.

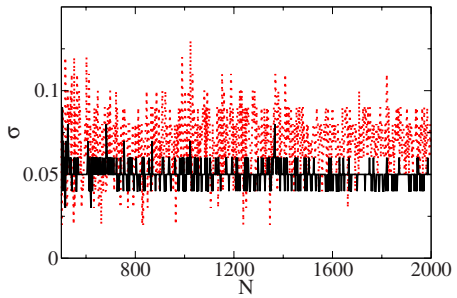

FIG. 5. (Color online) Width σ of the eigenvalue distributions W as a function of the dimension of the Hilbert space. The red dotted line corresponds to $q_c=0.5$, and the black solid line corresponds to $q_c=0.3$, being $\Delta q=0.1$ in both cases. Only values for $\nu>0.7$ were considered.

peaks for specific values of N where the opening contains the central discontinuity, that show both much higher and lower widths than for the $q_c=0.3$ case. In fact, we can identify the two peaks corresponding to the cases shown in the middle and lower panels of Fig. 4 (i.e., $N=602$ and $N=1782$). It is interesting to note that these peaks seem to be present also at the high N limit.

To see more clearly the scaling property of the distributions shown in Fig. 4, we have represented the same data, but now as a function of the decay rate and rescaled with the classical escape rates γ_{cl}. We show this in Fig. 6. From it, we can see that for openings with $q_c=0.3$ all distributions are almost the same, with a clear peak falling at $\Gamma\sim 0.1\sim\gamma_{cl}$. On the other hand, openings overlapping with the central discontinuity show eigenvalue distributions that are not rescalable to the ones corresponding to the previous nonoverlapping cases. Moreover, they are not rescalable among themselves. Fluctuations become the rule in these cases, ranging from peaks narrower than in the generic situations (like for $N=1782$) to distributions where no clear maximum can be found (like for $N=2048$ and $N=602$). This complements previous results found in the literature [9] for the open kicked rotator, where this scaling turned out to be universally valid.

We could associate this behavior with the fact that in the $q_c=0.5$ case the shortest periodic orbits survive the dissipation process and have a substantial role in the localization

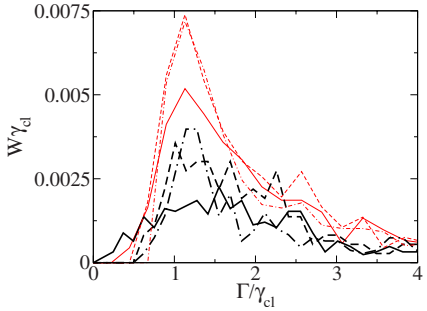

FIG. 6. (Color online) Same distributions as in Fig. 4, shown as a function of the decay rate and rescaled with γ_{cl}. Thin red lines correspond to $q_c=0.3$ and thick black lines correspond to $q_c=0.5$. Solid lines correspond to $N=2048$, dashed lines to $N=602$, and dotted-dashed lines to $N=1782$.

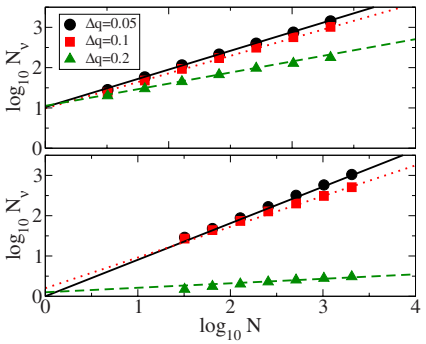

FIG. 7. (Color online) Logarithmic plot of the fraction of eigenstates N_ν for $\nu>0.3$, as a function of the dimension of the Hilbert space N. Lines correspond to the prediction given by the fractal Weyl law. Symbols correspond to the numerically calculated values. In the upper panel $q_c=0.3$ and in the lower panel $q_c=0.5$. In both cases black solid lines and circles correspond to $\Delta q=0.05$, red dotted lines and squares correspond to $\Delta q=0.1$, and green dashed lines and triangles correspond to $\Delta q=0.2$.

properties of resonances. In fact, there is numerical evidence that individual resonance eigenstates of an open quantum system present localization around unstable short periodic orbits in a similar way as their closed counterparts [14]. This so-called scarring phenomena could be important enough to make almost disappear the classical escape rate information from the quantum distributions. This last value is an average and now fluctuations become relevant. This includes situations where some particular quantization condition shrinks the distribution for a given N, as in the case of $N=1782$. In this new situation, the single quantum decay rates of resonances associated to given short periodic orbits could be singled out, and this would explain the multipeak structure of the corresponding distributions. When many orbits are relevant, and also longer ones, their decay rates combined could be more easily associated to a value that should better approximate the classical one.

Finally, we have checked whether the fractal Weyl law is verified or not by three different widths of the opening and for both representative q_c values. The logarithmic plots of the fraction of eigenstates for $\nu>0.3$ as a function of the dimension of the Hilbert space can be seen in Fig. 7. The lines correspond to the prediction of the fractal Weyl law $\ln(N_\nu)=\ln(N)(d_I-1)+A$ (where A is a constant). The symbols correspond to the numerically calculated values (see caption for more details). In all of these cases the slope is correctly described by the information dimension calculated from the area of the forward trapped set. We have adjusted the constant in order to fit the data. While in the left-hand panel the central discontinuity is not inside the opening and in the right-hand panel it is, we find that in both cases the agreement with the theoretical prediction is very good.

IV. CONCLUSIONS

In this work we have investigated the behavior of open piecewise linear maps. We have found that in the open baker map the role played by the central discontinuity is crucial.

First, we have made a brief study of the properties of the classical forward trapped sets. We have calculated the escape rates as a function of the location of the opening with respect to this singularity. We have found that when a cut along the p direction contains the discontinuity the information dimension of the repeller goes to the minimum. On the other hand, we have studied the behavior of the quantum map. We could verify that the distributions of the eigenvalues with the greatest classical information (i.e., with the greatest ν) show a similar behavior for different N values when the opening is located at a typical value of q (far from the influence of the central discontinuity). But when this is not the case the eigenvalues behave in a nonstandard way, showing distributions that cannot be rescaled to the previous ones, and not even among themselves for different N. For the less dense fractals corresponding to a smaller dimension ($q_c=0.5$) the role played by the shortest periodic orbits becomes relevant. This supports our conjecture that they are responsible for this behavior. Also, fluctuations connected with the quantization rules for these trajectories seem to be responsible for the great differences found for different values of N. Then, the results presented in this work could be of much relevance in order to understand the fundamental problem of scarring phenomena present in open quantum systems. We think that after developing a suitable probe of localization for this case, an interesting study will consist of checking if the peaks found in the W distribution correspond to short periodic orbits. Moreover, it will be very important to see if this behavior is also present in other types of systems, such as open kicked maps, for example. We will investigate on this in future studies [22]. Finally, it is remarkable that the fractal Weyl law is obeyed with great accuracy in all cases.

ACKNOWLEDGMENTS

Partial support by ANPCyT (PICT 25373), CONICET (PIP 6137), and UBACyT (X237) is gratefully acknowledged.

[1] W. H. Zurek and J. P. Paz, Phys. Rev. Lett. **72**, 2508 (1994); D. Braun, *Dissipative Quantum Chaos and Decoherence* (Springer-Verlag, New York, 2001).
[2] R. Akis, D. K. Ferry, and J. P. Bird, Phys. Rev. Lett. **79**, 123 (1997).
[3] W. Fang, A. Yamilov, and H. Cao, Phys. Rev. A **72**, 023815 (2005); T. Harayama, P. Davis, and K. S. Ikeda, Phys. Rev. Lett. **90**, 063901 (2003).
[4] J. Wiersig, Phys. Rev. Lett. **97**, 253901 (2006).
[5] J. U. Nockel and D. A. Stone, Nature (London) **385**, 45 (1997); J. Wiersig and M. Hentschel, Phys. Rev. A **73**, 031802(R) (2006); Phys. Rev. Lett. **100**, 033901 (2008).
[6] P. Gaspard, *Chaos, Scattering and Statistical Mechanics* (Cambridge University Press, Cambridge, 1998).
[7] C. Jung and T. H. Seligman, Phys. Rep. **285**, 77 (1997).
[8] W. T. Lu, S. Sridhar, and M. Zworski, Phys. Rev. Lett. **91**, 154101 (2003).
[9] D. L. Shepelyansky, Phys. Rev. E **77**, 015202(R) (2008).
[10] H. Schomerus and J. Tworzydlo, Phys. Rev. Lett. **93**, 154102 (2004).
[11] S. Nonnenmacher and M. Rubin, Nonlinearity **20**, 1387 (2007).
[12] S. Nonnenmacher and M. Zworski, J. Phys. A **38**, 10683 (2005).
[13] J. P. Keating, M. Novaes, S. D. Prado, and M. Sieber, Phys. Rev. Lett. **97**, 150406 (2006).
[14] D. Wisniacki and G. G. Carlo, Phys. Rev. E **77**, 045201(R) (2008).
[15] K. Zyczkowski and H.-J. Sommers, J. Phys. A **33**, 2045 (2000).
[16] M. Saraceno, Ann. Phys. **199**, 37 (1990); M. Saraceno and R. O. Vallejos, Chaos **6**, 193 (1996); A. Łoziński, P. Pakoński, and K. Zyczkowski, Phys. Rev. E **66**, 065201(R) (2002).
[17] J. R. Dorfman, *Introduction to Chaos in Nonequilibrium Statistical Mechanics* (Cambridge University Press, Cambridge, 1999).
[18] K. T. Alligood, T. D. Sauer, and J. A. Yorke, *Chaos, An Introduction to Dynamical Systems* (Springer-Verlag, New York, 1996).
[19] M. Saraceno and A. Voros, Physica D **79**, 206 (1994).
[20] A. J. Lichtenberg and M. A. Lieberman, *Regular and Chaotic Dynamics* (Springer-Verlag, New York, 1992).
[21] E. Ott, *Chaos in Dynamical Systems* (Cambridge University Press, Cambridge, 1993).
[22] J. Pedrosa, L. Ermann, G. G. Carlo, and D. A. Wisniacki (unpublished).